Polymer Journal (2011) 43, 186–193

www.nature.com/pj

ORIGINAL ARTICLE

# Synthesis and characterization of an exfoliated modified syndiotactic polystyrene/Mg–Al-layered double-hydroxide nanocomposite

Mehdi Jaymand

**This paper describes the synthesis and characterization of a controlled graft and block copolymerization onto syndiotactic polystyrene (sPS) using nitroxide-mediated living radical polymerization and the preparation of its polymer/layered double-hydroxide (LDH) nanocomposite. The graft and block copolymerization of styrene and *p*-methylstyrene were initiated with arylated sPS carrying 2,2,6,6-tetramethyl-1-piperidinyloxy groups as a macroinitiator. The structures of obtained graft and block copolymers were determined by $^1$H nuclear magnetic resonance and Fourier transform infrared spectroscopy. The MgAl(Cl)-LDH precursor was prepared with microwave irradiation using a mixed solution of $MgCl_2$ and $AlCl_3$, which was slowly pumped into decarbonated water. Thereafter, the surfactant-modified MgAl(SDBS) was obtained by the anion exchange reaction of MgAl(Cl)-LDH with sodium dodecyl benzene sulfate (SDBS). Finally, the sPS-*g*-(PS-*b*-PMS)/MgAl-LDH nanocomposite was prepared by a solution intercalation method. The exfoliated structure of the nanocomposite was probed by X-ray diffraction and transmission electron microscopy (TEM). Compared with pure sPS-*g*-(PS-*b*-PMS), the nanocomposite shows a much higher decomposition temperature and higher glass transition temperature.**
*Polymer Journal* (2011) **43,** 186–193; doi:10.1038/pj.2010.127; published online 15 December 2010

**Keywords:** functionalization; layered double hydroxide; living radical polymerization; modification; nanocomposite; syndiotactic polystyrene

## INTRODUCTION

Recently, there has been considerable interest in polymer/layered inorganic nanocomposites because of their different, often remarkably enhanced mechanical, thermal, electrical, optical and magnetic properties, which are rarely present in pure polymer or conventional composite. These enhanced properties are mainly attributed to the high degree of dispersion of layered inorganic compounds within the polymer matrix.[1–3] The layered materials include graphite and graphite oxide; metal chalcogenides such as molybdenum, titanium and lead sulfides; layered phosphates such as zirconium hydrogen phosphate; clays and layered silicates such as montmorillonite, hectorite and saponite; and layered double hydroxides (LDHs).[4,5] LDHs are a family of lamellar compounds that contain exchangeable ions in the interlayer space (anionic clays). The structure consists of brucite-like sheets with a typical thickness of 0.5 nm, in which the partial substitution of trivalent for divalent metallic ions results in a positive charge that is compensated by anions within the interlayer galleries. The general formula is $[M_{1-x}^{2+}M_x^{3+}(OH)_2]^{x+}A_{X/n}^{n-}\bullet mH_2O$, where $M^{2+}$ and $M^{3+}$ are the di- and trivalent metal cations, respectively, that occupy octahedral positions in the hydroxide layers, and $A^{n-}$ is an interlayer anion.[6,7] LDHs have been prepared with organic anions[8,9] and polymeric species anions.[10,11] LDHs have stronger interactions between the layers than silicates because of the higher charge density in the crystal structures that hinders the exfoliation of LDH nanolayers and the intercalation of polymer chains.[12] Accordingly, the intercalation of LDHs involves the organic modification of LDHs to expand the basal spacing and/or inorganic modification of polymers to graft anions onto polymers or monomers.[13]

Syndiotactic polystyrene (sPS) is an important engineering plastic and has excellent physical properties, such as a low dielectric constant, high chemical resistance, high hydrolytic resistance, high heat resistance and good dimensional stability.[14,15] However, although sPS has great physical properties, it has limited applications at low temperatures (lower than room temperature) because of its low compatibility and low impact resistance. Its glass transition temperature ($T_g$) at $\sim$100 °C is higher than room temperature. Many attempts have been made to characterize new materials and improve the physical and mechanical properties and processability of sPS.[16,17] Recently, several approaches to the modification of sPS, including the syndiotactic copolymerization of styrene with a second monomer, the postfunctionalization of sPS via sulfonation or Friedel–Crafts acylation reactions, and graft copolymerization have been developed to overcome these limitations.[18–21]

Laboratory of Polymer, Faculty of Chemistry, Payame Noor University, Tabriz, Iran
Correspondence: Dr M Jaymand, Laboratory of Polymer, Faculty of Chemistry, Payame Noor University, Tabriz 5158654778, Iran.
E-mail: m_jaymand@yahoo.com or m.jaymand@gmail.com
Received 24 August 2010; revised 18 October 2010; accepted 30 October 2010; published online 15 December 2010

Stable free-radical polymerization, which is often also described as nitroxide-mediated polymerization, is well established as a controlled radical polymerization methodology.[22,23] The systematic variation of monomer weight to the moles of the initiator leads to predictable molecular weights and relatively low polydispersities ($Mw/Mn \sim 1.20$). Stable free-radical polymerization offers functional group tolerance, which is typical of radical polymerizations. This tolerance provides versatility that is often not easily achieved with other living polymerization techniques, and less stringent purification techniques are required than those for living anionic polymerization. Moreover, SFPR enables the synthesis of block, graft, star and hyperbranched topologies in a manner similar to other living polymerization processes.[24–27]

In this study, TEMPO (2,2,6,6-tetramethyl-1-piperidinyloxy) is reduced to 1-hydroxy-2,2,6,6-tetramethylpiperidine with sodium ascorbate. This functional nitroxyl compound was coupled with the α-phenyl-chloro-acetylated sPS that was synthesized previously. This macroinitiator (sPS–TEMPO) is used for nitroxide-mediated radical polymerization in the presence of styrene and *p*-methylstyrene monomers to prepare grafts and block copolymers. MgAl(Cl)-LDH was prepared by the coprecipitation method with microwave irradiation. Surfactant-modified MgAl(SDBS) was obtained by the ion-exchange process by treating MgAl(Cl) with sodium dodecyl benzene sulfate (SDBS). The sPS-*g*-(PS-*b*-PMS)/MgAl-LDH nanocomposite was prepared using a solution intercalation method.

## EXPERIMENTAL PROCEDURE

### Materials

TEMPO and α-phenyl-chloro-acetylated sPS were prepared in our laboratory. Styrene and *p*-methylstyrene monomers were supplied by Merck (Darmstadt, Germany) and were distilled under vacuum before use. Xylene (Merck) was dried by refluxing over sodium and distilled under argon before use. Sodium ascorbate, $MgCl_2{\cdot}6H_2O$, $AlCl_3{\cdot}6H_2O$, NaOH and SDBS were supplied by Merck and used without further purification. All other reagents were purified according to the literature.

### Preparation of TEMPO–OH by reducing TEMPO

TEMPO (0.25 g, 1.6 mmol) was suspended in a solution of sodium ascorbate (0.503 g, 2.65 mmol) in water (5 ml) and shaken vigorously until it was completely decolorized (~30 min). The resulting suspension was extracted with ether. Thereafter, the ether extracts were washed with water and brine, dried (using $Na_2SO_4$) and evaporated under reduced pressure to produce a crude product (Scheme 1).

### Synthesis of the sPS–TEMPO macroinitiator

In a three-neck round-bottom flask equipped with a condenser, dropping funnel, gas inlet/outlet and a magnetic stirrer, 51 mg (0.33 mmol) of TEMPO–OH was dissolved in anhydrous *N*,*N*-dimethylformamide (3 ml) and added under $N_2$ atmosphere to 11 mg (0.45 mmol) of hexane-washed NaH (from 60% suspension in oil). The mixture was stirred for 30 min, and then 1 g of α-phenyl-chloroacetylated sPS was added under $N_2$ and refluxed for 24 h. The reaction was terminated by pouring the contents of the flask into a large amount of acidic methanol. The white solid was filtered and dried under vacuum (Scheme 2).

### Nitroxide-mediated living radical polymerization (NMRP) of styrene and *p*-methylstyrene onto sPS

sPS–TEMPO macroinitiator (0.50 g) and 5 ml (43.7 mmol) of styrene were placed in an ampoule degassed with several freeze–pump–thaw cycles and sealed off under vacuum and placed in an oil bath at 125 °C. During the reaction, the viscosity of the mixture was observed to gradually increase. After 10 h, the mixture was dissolved in 10 ml of $CH_2Cl_2$ and precipitated in 50 ml of hexane for 24 h and then reprecipitated from $CH_2Cl_2$ into 50 ml of methanol. The crude product was then dried under vacuum. In a typical experiment, the reaction was carried out in the presence of *p*-methylstyrene. The obtained powders were extracted three times with cyclohexane at 30 °C to remove PS (polystyrene) and poly *p*-methylstyrene (PMS) homopolymers (Scheme 3).

### Preparation of MgAl(Cl)-LDH

A mixed solution of magnesium chloride (0.75 M) and aluminum chloride (0.25 M) was slowly pumped into 150 ml of decarbonated water under flowing $N_2$ with vigorous stirring at a constant pH of $8.0 \pm 0.2$, which was adjusted by the simultaneous dropwise addition of NaOH solution (0.5 M). The resulting gels were treated in a microwave autoclave for 8 h operating at 2.45 GHz with a maximum power of 600 W. The solids were recovered by decantation and washed several times with distilled water and filtered.

### Preparation of surfactant-modified MgAl(SDBS)

Anionic surfactants are often used to intercalate LDHs to expand the basal spacing and make them compatible with the organic matrix. To prepare the polymer/LDH nanocomposite, we first modified MgAl(Cl)-LDH with SDBS. Surfactant-modified MgAl(SDBS) was obtained by the anion exchange reaction of 0.5 g of MgAl(Cl) with 50 ml of SDBS (0.1 M) at 60 °C. For this purpose, 0.5 g of MgAl(Cl) was dispersed into 100 ml of decarbonated water by ultrasonic vibration for 20 min. Thereafter, 50 ml of SDBS (0.1 M) was slowly pumped into the suspension, and the obtained slurry was stirred vigorously with a magnetic pellet for 24 h at 60 °C, after which the solids were recovered by decantation and washed several times with distilled water and filtration.

### Preparation of the sPS-*g*-(PS-*b*-PMS)/LDH nanocomposite

The sPS-*g*-(PS-*b*-PMS)/MgAl-LDH nanocomposite was prepared by a solution intercalation method. A desired amount (5 wt%) of MgAl(SDBS) was first refluxed in 100 ml of xylene for 24 h under flowing $N_2$. Thereafter, 1.0 g of sPS-*g*-(PS-*b*-PMS) was added to the MgAl(SDBS) suspension. After stirring for 3 h at 90 °C, the mixture was poured into 300 ml of methanol for rapid precipitation. The precipitate was filtered and dried at 60 °C under vacuum for 2 days.

### Characterization

Fourier transform infrared (FT-IR) spectra of the samples were obtained on a Shimadzu 8101M FT-IR (Shimadzu, Kyoto, Japan). The samples were prepared by grinding the dry powders with KBr and compressing the mixture to form disks. The disks were stored in a desiccator to avoid moisture absorption. The spectra were recorded at room temperature. $^1$H nuclear magnetic resonance (NMR) spectra were obtained at 25 °C on an FT-NMR (400 MHz) Brucker spectrometer (Brucker, Ettlingen, Germany). The sample for $^1$H-NMR spectroscopy was prepared by dissolving about 10 mg of products in 5 ml of deuterated chloroform. The thermal properties of the copolymers and nanocomposite were obtained with a TGA-PL STA 1640 (Polymer Laboratories, Shropshire, UK). About 10 mg of the sample was heated between 25 and 600 °C at a rate of 10 °C min$^{-1}$ under flowing nitrogen. Differential scanning calorimetry analyses were performed with a NETZSCH (Selb, Germany)—DSC 200 F3 Maia. The sample was first heated to 200 °C and then allowed to cool

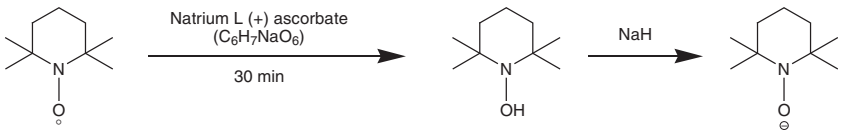


**Scheme 1** Preparation of TEMPO–OH by reduction of TEMPO (2,2,6,6-tetramethyl-1-piperidinyloxy).

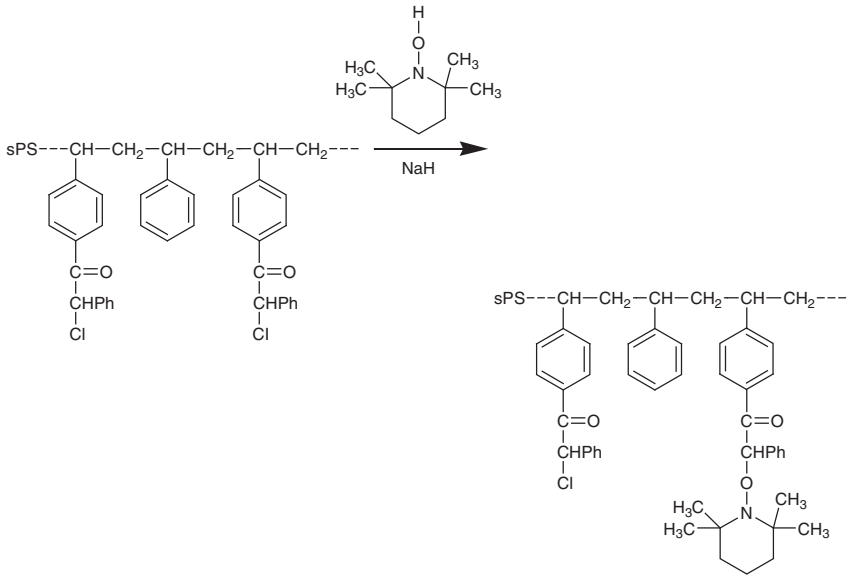


**Scheme 2** Synthesis of the syndiotactic polystyrene (sPS)–TEMPO (2,2,6,6-tetramethyl-1-piperidinyloxy) macroinitiator.

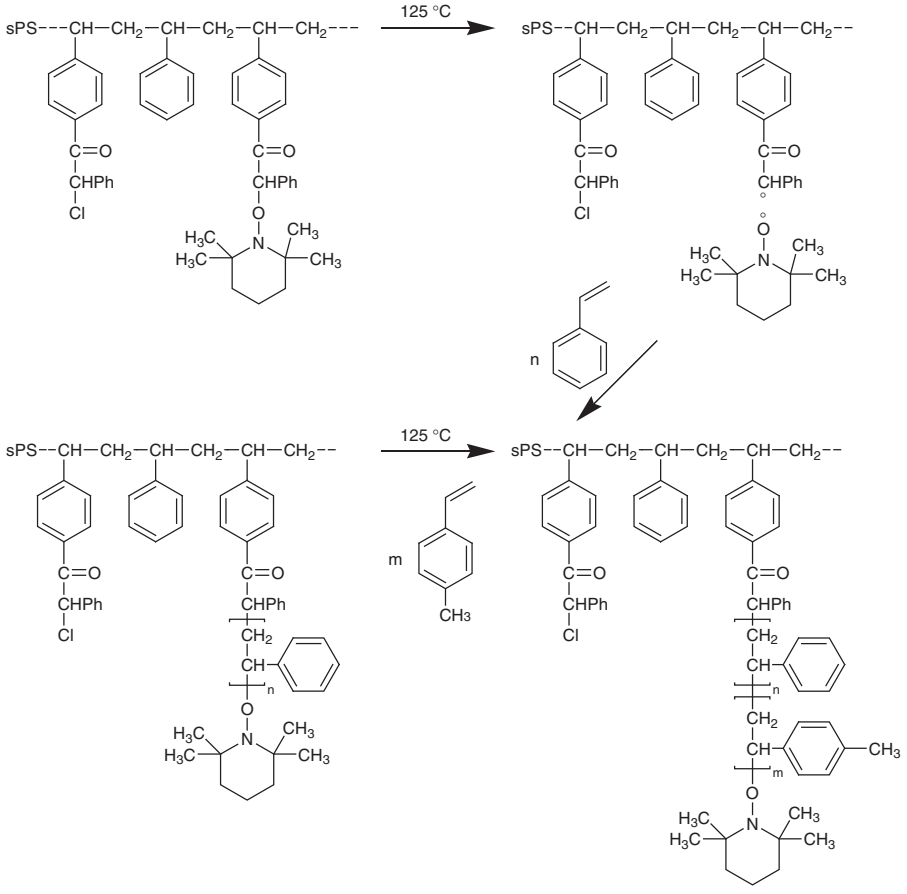


**Scheme 3** Graft copolymerization of styrene and *p*-methylstyrene onto syndiotactic polystyrene.

for 5 min to eliminate the thermal history. Thereafte, the sample was reheated to 200 °C at a rate of 10 °C min$^{-1}$. The entire test was performed under nitrogen purging at a flow rate of 50 ml min$^{-1}$. Transmission electron microscopy (TEM) was performed on a Philips EM208 microscope (Phillips, Eindhoven, Netherlands) with a 100 kV accelerating voltage. X-ray diffraction (XRD) spectra were obtained with a Siemens D 5000 (Aubrey, Texas, USA), X-ray generator (Cu$K_\alpha$ radiation with $\lambda$=1.5406 Å) with a 2$\theta$ scan range of 2–80° at room temperature.

## RESULTS AND DISCUSSION

### Synthesis of the sPS–TEMPO macroinitiator

Figure 1 shows the FT-IR spectra of the α-phenyl-chloroacetylated sPS (a) and the sPS–TEMPO macroinitiator (b). The sPS–TEMPO macroinitiator was prepared by the reaction of TEMPO–OH with α-phenyl-chloroacetylated sPS. The FT-IR spectrum of the sPS–TEMPO macroinitiator demonstrates an absorption band at 1382 $cm^{-1}$, which is attributed to the methyl bond of TEMPO. The stretching bonds of C–N and N–O of TEMPO are absent in the FT-IR spectrum of the macroinitiator because these peaks overlap with the peaks from sPS.

### NMRP of styrene and *p*-methylstyrene onto sPS

At first, to produce active sites on sPS, TEMPO was added to sPS. Then, to generate active sites on sPS, after the α-chloro-acetylation of sPS, TEMPO–OH was reacted with α-ph-ch-sPS to produce the sPS–TEMPO macroinitiator. A comparison of the $^1$H-NMR spectrum of α-ph-ch-sPS with the $^1$H-NMR spectrum of sPS–TEMPO indicates that, during the reaction, because the chemical shifts of CH–O and CH–Cl are similar, there are no changes in the chemical shifts of CH–O, whereas the functional group of TEMPO appears with characteristic signals at 0.50–1.58 p.p.m. (Figure 2). The thermal homolytic scission of the C–O bond of the aminoxy moiety of the sPS–TEMPO takes place at 125 °C and causes the radical polymerization of styrene and *p*-methylstyrene to yield the controlled graft (sPS-*g*-PS) and block [sPS-g-(PS-*b*-PMS)] copolymerization.[28,29] The bond dissociation is considered to be reversible.

To successfully carry out this copolymerization, it was necessary to perform this reaction at a temperature at which spontaneous thermal polymerization occurs and under conditions in which the polymerization is living and controlled. For comparison, the blank experiments that proceed in the absence of TEMPO into sPS are also included. In this case, no homopolystyrene or poly *p*-methylstyrene was formed in the absence of the macroinitiator under identical NMRP conditions. This suggests that the possibility of formation of the homopolymer in the grafting reaction can be excluded in this study, and it demonstrates that the polymerization is living. The $^1$H-NMR spectra of the products (Figure 3) indicate the formation of controlled graft (sPS-*g*-PS) and block [sPS-*g*-(PS-*b*-PMS)] copolymers, because the chemical shifts at 6.39–7.25 p.p.m. represent aromatic protons, and those at 1.2–2.1 p.p.m. represent aliphatic protons. Because the ratio of aliphatic hydrogens to aromatic hydrogens is 3:5, there is an increase in the integration intensity of aromatic hydrogen in the $^1$H-NMR spectra. The functional group of TEMPO appears with characteristic signals at 0.50–1.38 p.p.m. The $^1$H-NMR spectra show that the functional groups of the TEMPO were retained at the end of the polymer chains, which provides strong evidence that the NMRP reaction occurred.

### Characterization of MgAl(Cl) and surfactant-modified MgAl(SDBS)

The XRD patterns of MgAl(Cl) and surfactant-modified MgAl(SDBS) are shown in Figure 4. The XRD pattern of MgAl(Cl) (Figure 4a) can be indexed in a hexagonal lattice with an R-3m rhombohedral symmetry, which is commonly used for the description of the LDH structure. The basal spacing of the MgAl(Cl) sample is 0.78 nm. The basal spacing of the MgAl(SDBS) sample increases to 1.92 nm after the $Cl^-$ ions in the MgAl(Cl) sample are exchanged by SDBS, which indicates that the SDBS anions have been intercalated in the MgAl-LDH layers.

The morphologies of MgAl(Cl) and MgAl(SDBS) are shown in Figure 5. The scanning electron microscopy images of MgAl(Cl) ($a_1$, $a_2$) show sheet-like structures for the nanoparticles, which will give a small surface area. The morphologies of MgAl(SDBS) ($b_1$, $b_2$) show

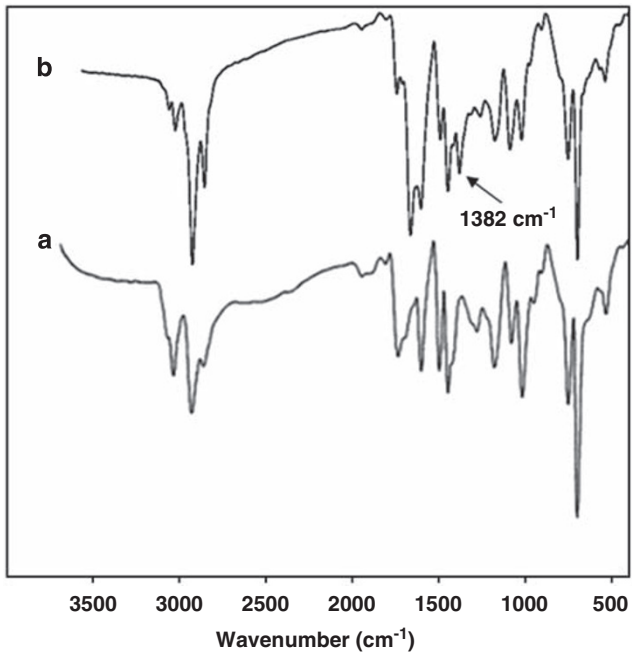


**Figure 1** Fourier transform infrared spectra of α-phenyl-chloroacetylated syndiotactic polystyrene (sPS) (**a**) and the sPS–TEMPO (2,2,6,6-tetramethyl-1-piperidinyloxy) macroinitiator (**b**).

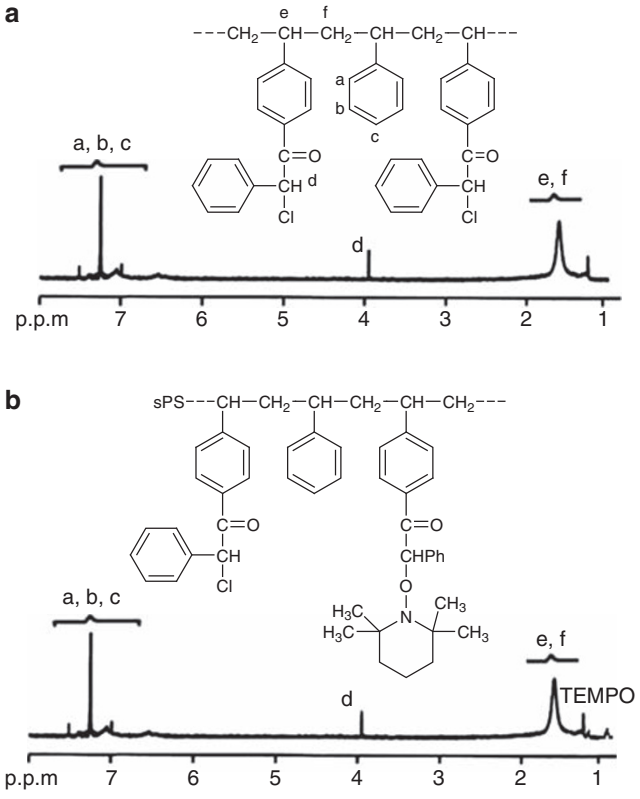


**Figure 2** $^1$H nuclear magnetic resonance spectra of α-phenyl-chloroacetylated syndiotactic polystyrene (sPS) (**a**) and the sPS—TEMPO (2,2,6,6-tetramethyl-1-piperidinyloxy) macroinitiator (**b**).

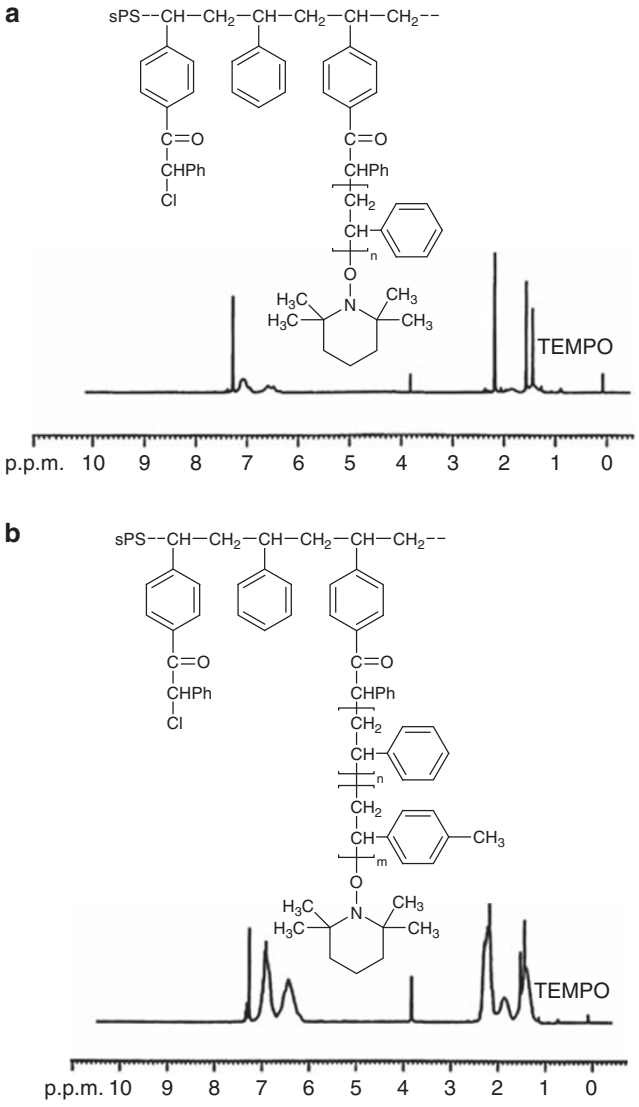


**Figure 3** $^1$H nuclear magnetic resonance spectra of sPS-*g*-PS (**a**) and sPS-*g*-(PS-*b*-PMS) (**b**).

homogeneously distributed particles, which give a relatively large surface area. This fact is especially important in preparing the polymeric nanocomposite.

The FT-IR spectra of MgAl(Cl) and MgAl(SDBS) are shown in Figure 6. The MgAl(Cl) sample has a broad adsorption band at around 3445 $cm^{-1}$ because of stretching of the O–H bonds of the hydroxyl groups of LDH. The corresponding δ (H–OH) vibration appears at about 1632 $cm^{-1}$. The lattice vibration bands from the M–O and O–M–O (M=Mg, Al) groups appear in the 400–800 $cm^{-1}$ region. The intercalation of SDBS instead of $Cl^-$ ions can be confirmed by the C–H stretching vibration at 2856, 2925 and 2958 $cm^{-1}$ and the stretching vibration of the sulfate group at 1041 $cm^{-1}$.

### Characterization of the exfoliated sPS-*g*-(PS-*b*-PMS)/MgAl-LDH nanocomposite

XRD provides information on the changes of the interlayer spacing of the LDH on the formation of the nanocomposite. The formation of an intercalated structure should result in a decrease in $2\theta$, which would indicate an increase in the d-spacing. The formation of an exfoliated

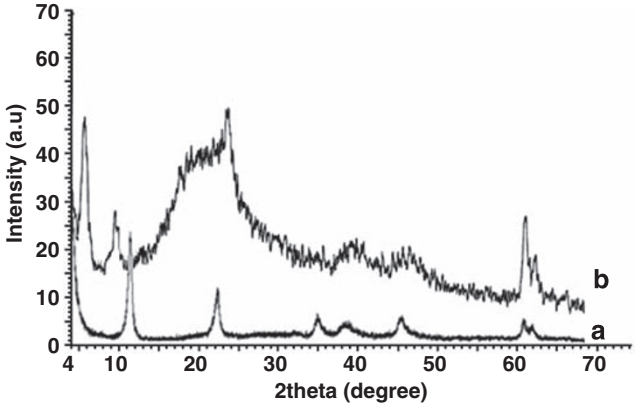


**Figure 4** X-ray diffraction patterns of MgAl(Cl) (**a**) and MgAl(SDBS) (**b**).

structure usually results in the complete loss of registry between the LDH layers, and thus no peak can be seen in the XRD trace. In some cases, a disordered immiscible system is obtained, which also shows no peaks; hence, the absence of an XRD peak cannot be taken as definitive evidence of the formation of an exfoliated nanocomposite, and additional evidence, usually TEM images, is required.[30–32] The XRD patterns of the sPS-*g*-(PS-*b*-PMS)/MgAl-LDH nanocomposite in the range of $2\theta$=2–70° are shown in Figure 7. For the nanocomposite, no peaks are observed, which could mean that either an exfoliated or an immiscible nanocomposite has been formed.

The XRD results give useful information on the state of organo-LDH in the polymer, but do not provide a complete picture of the morphology. TEM is required to complement this information to enable the evaluation of the dispersion of LDH in the polymer matrix. Usually, both low-magnification images, to show whether the LDH is well dispersed, and high-magnification images, to provide an identification of the morphology, are necessary. The morphologies of the sPS-*g*-(PS-*b*-PMS)/MgAl-LDH nanocomposite with 5wt% organo-LDH loading are shown in Figure 8. Light regions represent the polymer matrix, and dark lines indicate LDH layers. At lower magnification (Figure 8a), the boundaries between the matrix and filler particles are visible, which indicates that a portion of the matrix is not influenced by the filler. However, the particles contain much of the matrix as well. At higher magnification (Figure 8b), the delamination of LDH(SDBS) into individual layers can be clearly seen in the filler particle region.

The FT-IR spectra of pure sPS-*g*-(PS-*b*-PMS) (Figure 9a) show the characteristic absorption bands due to the stretching vibration of C–H in the 3100–2850 $cm^{-1}$ region, weak aromatic overtones and combination bands in the 2100–1650 $cm^{-1}$ region, C=C stretching vibrations at 1606 and 1510 $cm^{-1}$, $-CH_2$ bending vibrations at 1445 and 1372 $cm^{-1}$, and γ(C–H) in the aromatic ring at 752 and 702 $cm^{-1}$. Apparently, the FT-IR spectrum of the sPS-*g*-(PS-*b*-PMS)/MgAl-LDH nanocomposite (Figure 9b) shows the combination of samples MgAl(SDBS) and sPS-*g*-(PS-*b*-PMS), in which the absorption bands of the O–H stretching vibrations are at ~3450 $cm^{-1}$. These FT-IR assignments verify that the LDH layers have been doped into the polymer matrix during the precipitation process, and thus form the sPS-*g*-(PS-*b*-PMS)/LDH nanocomposite.

### Glass transition of the sPS-*g*-(PS-*b*-PMS) and sPS-*g*-(PS-*b*-PMS)/LDH nanocomposites

Additional evidence on the effectiveness of graft copolymerization was also obtained from the differential scanning calorimetry data. The

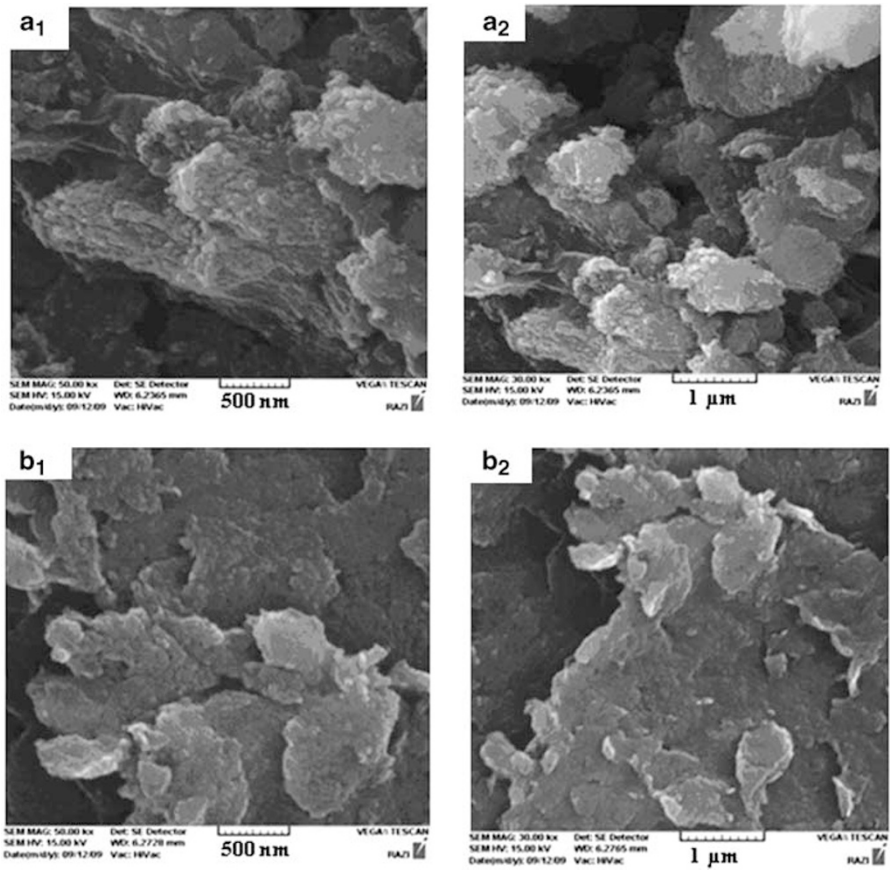


**Figure 5** Scanning electron microscop images of MgAl(Cl) (**$a_1$, $a_2$**) and MgAl(SDBS) (**$b_1$, $b_2$**) at different magnifications.

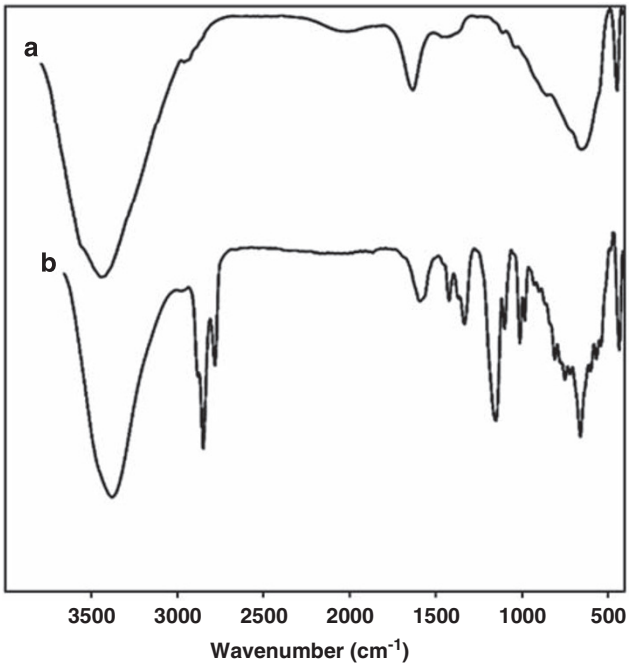


**Figure 6** Fourier transform infrared spectra of MgAl(Cl) (**a**) and MgAl(SDBS) (**b**).

graft copolymer studied in this work consists of an sPS backbone carrying amorphous atactic polystyrene and poly *p*-methylstyrene. The presence of graft segments should affect the melting behavior of the sPS backbone. The random incorporation of non-crystallizable

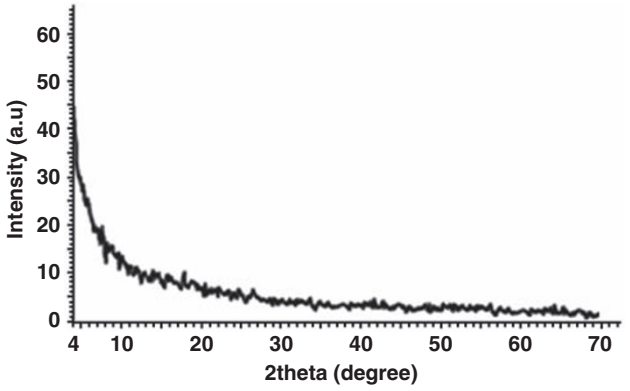


**Figure 7** X-ray diffraction patterns of the sPS-*g*-(PS-*b*-PMS)/MgAl-LDH nanocomposite.

monomer units into the backbone of a semicrystalline polymer has a marked effect on the thermodynamics and kinetics of crystallization. Relative to the behavior observed with the homopolymer, the crystallizable copolymer usually exhibits a low melting temperature, low degree of crystallinity and a significant decrease in the overall rate of crystallization.[33] The $T_g$ data also help in understanding the effects of constituent groups on the movement of polymer chains. It is clear from Figure 10 that the $T_g$ values of the modified polymers depend on the graft copolymerization. This is easy to understand because the substituent groups reduce the mobility of the polymer chain and thereby increase the $T_g$ values.

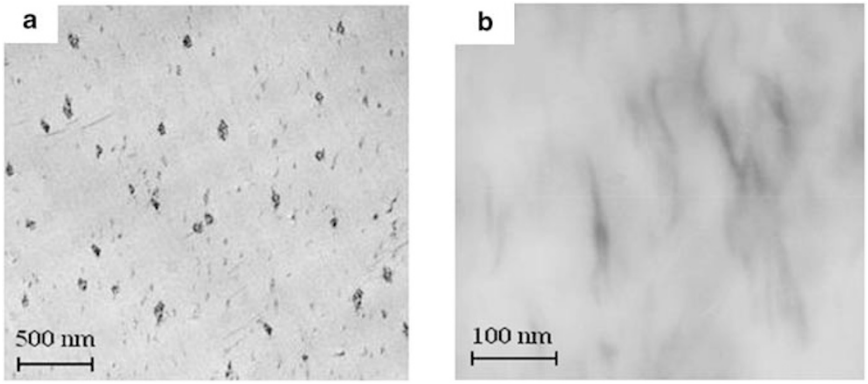


**Figure 8** Transmission electron microscope image of the sPS-*g*-(PS-*b*-PMS)/MgAl-LDH nanocomposite at low magnification (**a**) and at high magnification (**b**).

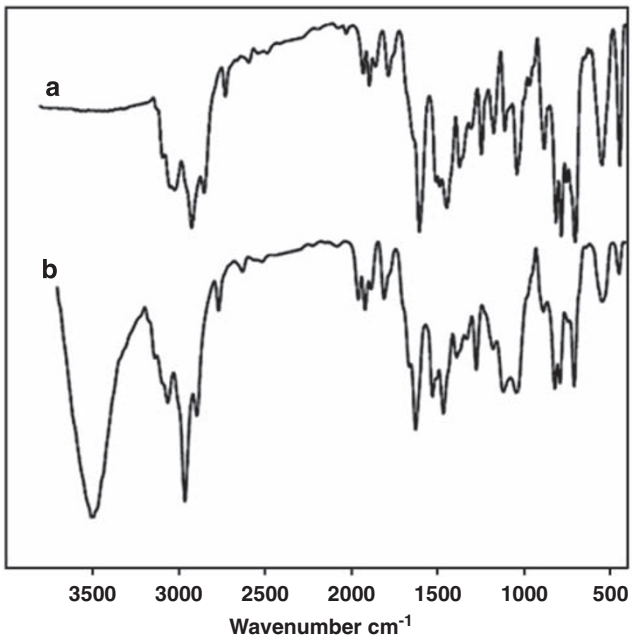


**Figure 9** Fourier transform infrared spectra of pure sPS-*g*-(PS-*b*-PMS) (**a**) and the sPS-*g*-(PS-*b*-PMS)/LDH nanocomposite (**b**).

The differential scanning calorimetry curves of the sPS, sPS-*g*-(PS-*b*-PMS) and sPS-*g*-(PS-*b*-PMS)/LDH nanocomposites are shown in Figure 10. For pure sPS, $T_g$ and $T_m$ were around 98.4 and 270 °C, respectively. The $T_g$ of sPS-*g*-(PS-*b*-PMS) is 99.2 °C, and the $T_g$ of the sPS-*g*-(PS-*b*-PMS)/LDH nanocomposite (5 wt% LDH) is 103.4 °C, which is slightly higher than that of pure sPS-*g*-(PS-*b*-PMS). In addition, the $T_g$ was also increased slightly in the presence of LDH. The increased $T_g$ resulted from the restricted segmental motion of the polymer chain at the organic/inorganic interface because of the confinement of sPS-*g*-(PS-*b*-PMS) chains between the LDH layers. This result also indicates that the nanoplatelets were reasonably well exfoliated and dispersed. It was also reported in the literature that the majority of the other well-dispersed polymer nanocomposites also exhibit higher $T_g$ values than their corresponding pristine polymers.

**Thermal stability of the sPS-*g*-(PS-*b*-PMS)/LDH nanocomposite**

The characteristic thermogravimetric analysis curves of the sPS-*g*-(PS-*b*-PMS) and sPS-*g*-(PS-*b*-PMS)/LDH nanocomposites are shown in Figure 11 and Table 1. The thermogravimetric analysis results indicate an improvement in the thermal stability of the sPS-*g*-(PS-*b*-PMS)/

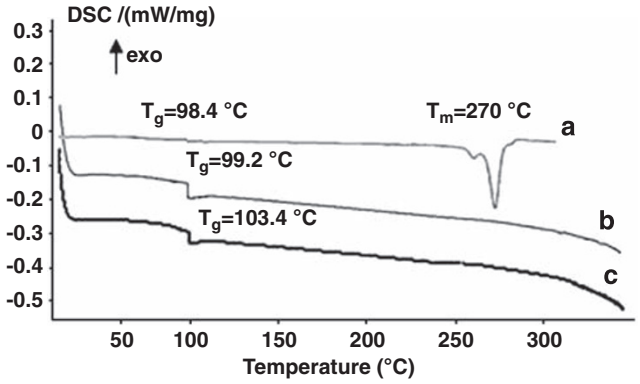


**Figure 10** Differential scanning calorimeter traces of the neat syndiotactic polystyrene (sPS) (**a**), sPS-*g*-(PS-*b*-PMS) (**b**) and the sPS-*g*-(PS-*b*-PMS)/LDH nanocomposite (**c**).

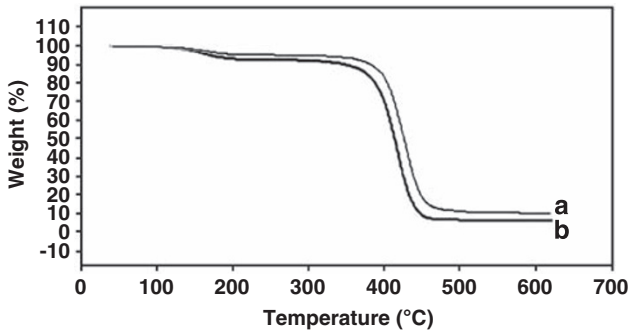


**Figure 11** Thermogravimetric analysis of the sPS-*g*-(PS-*b*-PMS)/LDH nanocomposite (**a**) and pure sPS-*g*-(PS-*b*-PMS) (**b**).

LDH nanocomposite (5 wt% LDH) compared with that of neat sPS-*g*-(PS-*b*-PMS). Data on the onset of the degradation temperatures (at which 10% degradation occurs, symbol $T_{0.1}$), the midpoint of the degradation temperatures (at which 50% degradation occurs, symbol $T_{0.5}$) and the residue that was at 600 °C showed higher temperatures in the sPS-*g*-(PS-*b*-PMS)/LDH nanocomposite than in the neat sPS-*g*-(PS-*b*-PMS). The increase in thermal stability is mainly attributed to the homogeneous dispersion of MgAl(SDBS) in the sPS-*g*-(PS-*b*-PMS) matrix, as depicted in TEM images. During the course of thermal decomposition, the homogeneously dispersed MgAl(SDBS) forms protective oxide layers on the nanocomposite surface, which impedes the burning process by reducing the oxygen supply to the bulk and preventing the emission of degraded small gaseous

**Table 1 TGA results of sPS-*g*-(PS-*b*-PMS) and sPS-*g*-(PS-*b*-PMS)/LDH nanocomposite**

| *Samples* | $T_{0.1\,(°C)}$ | $T_{0.5\,(°C)}$ | *Residue at 600°C (wt%)* |
|---|---|---|---|
| sPS-*g*-(PS-*b*-PMS) | 353 | 418 | 6.21 |
| sPS-*g*-(PS-*b*-PMS)/LDH | 382 | 431 | 11.26 |

Abbreviations: LDH, layered double hydroxide; PMS, poly *p*-methylstyrene; PS, polystyrene; sPS, syndiotactic polystyrene; TGA, thermogravimetric analysis.

molecules.[34] Moreover, according to Figure 11a, we can conclude that the weight loss of the nanocomposite between 150 and 400 °C is accelerated, mainly because of the dehydration reaction of MgAl(SDBS), followed by the early degradation of the SDBS molecules.[35]

## CONCLUSION

TEMPO-terminated syndiotactic polystyrene (sPS–TEMPO) was prepared by reacting chloroacetylated sPS with sodium 4-oxy-TEMPO derived from TEMPO–OH. The macroinitiator sPS–TEMPO initiates the 'living' free-radical polymerization of styrene and *p*-methylstyrene monomers to yield the controlled graft (sPS-*g*-PS) and block (sPS-*g*-(PS-*b*-PMS)) copolymers. MgAl(Cl)-LDH was prepared with microwave irradiation, after which the surfactant-modified MgAl(SDBS) was obtained by the anion exchange reaction of MgAl(Cl)-LDH with SDBS. The exfoliated sPS-*g*-(PS-*b*-PMS)/LDH nanocomposite (5 wt% LDH) was prepared by a solution intercalation method. The XRD and TEM data showed that the exfoliation of LDH in solution involves two steps of solvent swelling and layer-breaking processes during refluxing. The thermal stability and $T_g$ of the sPS-*g*-(PS-*b*-PMS)/LDH nanocomposite improved considerably, relative to that of pure sPS-*g*-(PS-*b*-PMS). The unique properties of the nanocomposite result from the strong interactions between the LDH layers and polymeric chains.

## ABBREVIATIONS

DSC, differential scanning calorimetry; LDH, layered double hydroxide; NMRP, nitroxide-mediated living radical polymerization; PMS, poly *p*-methylstyrene; PS, polystyrene; SDBS, sodium dodecyl benzene sulfate; sPS, syndiotactic polystyrene; TEM, transmission electron microscopy; $T_g$, glass transition temperature; TEMPO, 2,2,6,6-tetramethylpiperidinyloxy; XRD, X-ray diffraction.

## ACKNOWLEDGEMENTS

I express my gratitude to the Bonyade Melli Nokhbeghan Institute and Payame Noor University for supporting this project.

1 Kotal, M., Srivastavaa, S. K. & Bhowmick, A. K. Thermoplastic polyurethane and nitrile butadiene rubber blends with layered double hydroxide nanocomposites by solution blending. *Polym. Int.* **59,** 2–10 (2010).
2 Costache, M. C., Wang, D., Heidecker, M. J., Manias, E. & Wilkie, C. A. The thermal degradation of poly(methyl methacrylate) nanocomposites with montmorillonite, layered double hydroxides and carbon nanotubes. *Polym. Adv. Technol.* **17,** 272–280 (2006).
3 Jaymand, M. Surface modification of montmorillonite with novel modifier and preparation of polystyrene/montmorillonite nanocomposite by *in situ* radical polymerization. *J. Polym. Res.* (e-pub ahead of print 17 September 2010).
4 Matusinović, Z., Rogošić, M. & Šipušic, J. Synthesis and characterization of poly (styrene-*co*-methyl methacrylate)/layered double hydroxide nanocomposites via *in situ* polymerization. *Polym. Degrad. Stabil.* **94,** 95–101 (2009).
5 Acharya, H., Srivastava, S. K. & Bhowmick, A. K. Synthesis of partially exfoliated EPDM/LDH nanocomposites by solution intercalation: structural characterization and properties. *Compos. Sci. Technol.* **67,** 2807–2816 (2007).
6 Ardanuy, M., Velasco, J. I., Realinho, V., Arenćn, D. & Martnez, A. B. Non-isothermal crystallization kinetics and activity of filler in polypropylene/Mg–Al layered double hydroxide nanocomposites. *Thermochim. Acta.* **479,** 45–52 (2008).
7 Das, J., Das, D. & Paridaa, K. M. Preparation and characterization of Mg-Al hydrotalcite-like compounds containing cerium. *J. Colloid. Interf. Sci.* **301,** 569–574 (2006).
8 Rivera, J. A., Fetter, G., Jiménez, Y., Xochipa, M. M. & Bosch, P. Nickel distribution in (Ni,Mg)/Al-layered double hydroxides. *Appl. Catal.* **316,** 207–211 (2007).
9 Vreysen, S. & Maes, A. Adsorption mechanism of humic and fulvic acid onto Mg/Al layered double hydroxides. *Appl. Clay Sci.* **38,** 237–249 (2008).
10 Gillman, G. P., Noble, M. A. & Raven, M. D. Anion substitution of nitrate-saturated layered double hydroxide of Mg and Al. *Appl. Clay Sci.* **38,** 179–186 (2008).
11 Moujahid, E. M., Besse, J. P. & Leroux, F. Synthesis and characterization of a polystyrene sulfonate layered double hydroxide nanocomposite. *In-situ* polymerization vs polymer incorporation. *J. Mater. Chem.* **12,** 3324–3330 (2002).
12 Kuila, T., Srivastava, S. K., Bhowmick, A. K. & Saxena, A. K. Thermoplastic polyolefin based polymer-blend-layered double hydroxide nanocomposites. *Compos. Sci. Technol.* **68,** 3234–3239 (2008).
13 Qiu, L., Chen, W. & Qu, B. Structural characterisation and thermal properties of exfoliated polystyrene/ZnAl layered double hydroxide nanocomposites prepared via solution intercalation. *Polym. Degrad. Stabil.* **87,** 433–440 (2005).
14 Ishihara, N., Seimiya, T., Kuramoto, M. & Uoi, M. Crystalline syndiotactic polystyrene. *Macromolecules* **19,** 2464–2465 (1986).
15 Lyu, Y. Y., Byun, Y., Yim, J. H., Chang, S., Lee, S. Y., Pu, L. S. & Lee, I. M. Novel metallocene catalysts for syndiotactic polystyrene. *Eur. Polym. J.* **40,** 1051–1056 (2004).
16 Gao, Y. & Li, H. M. Synthesis of syndiotactic-polystyrene-graft-poly(methyl methacrylate) and syndiotactic-polystyrene-graft-atactic-polystyrene by atom transfer radical polymerizatio. *Eur. Polym. J.* **41,** 2329–2334 (2005).
17 Gao, Y. & Li, H. M. Synthesis and characterization of acetylated syndiotactic polystyrene. *Polym. Int.* **53,** 1436–1441 (2004).
18 Shin, J., Jensen, S. M., Ju, J. H., Lee, S., Xue, Z. G., Noh, S. K. & Bae, C. Controlled functionalization of crystalline polystyrenes via activation of aromatic C-H bonds. *Macromolecules* **40,** 8600–8608 (2007).
19 Gao, Y., Li, H. M. & Wang, X. Y. Synthesis and characterization of syndiotactic polystyrene-graft-poly (glycidyl methacrylate) copolymer by atom transfer radical polymerization. *Eur. Polym. J.* **43,** 1258–1266 (2007).
20 Li, H. M., Chen, H. B., Shen, Z. G. & Lin, S. A. Preparation and characterization of maleic anhydride-functionalized syndiotactic polystyrene. *Polymer* **43,** 5455–5461 (2002).
21 Picchioni, F., Passaglia, E., Ruggeri, G. & Ciardelli, F. Blends of Syndiotactic Polystyrene with SBS Triblock Copolymers. *Macromol. Chem. Phys.* **202,** 2142–2147 (2001).
22 Mather, B., Lizotte, J. & Long, T. Synthesis of Chain End Functionalized Multiple Hydrogen Bonded Polystyrenes and Poly(alkyl acrylates) Using Controlled Radical Polymerization. *Macromolecules* **37,** 9331–9337 (2004).
23 Cruz, B. J., Guerra, S. E., Lubián, T. J., Santos, G. R., Carpy, L. B. & Bárcenas, L. G. Controlled grafting-from of polystyrene on polybutadiene: mechanism and spectroscopic evidence of the functionalization of polybutadiene with 4-Oxo-TEMPO. *Macromol. Chem. Phys.* **209,** 2268–2283 (2008).
24 Jaymand, M. Synthesis and characterization of conductive polyaniline-modified polymers via nitroxide mediated radical polymerization. *Polymer (Korea)* **34,** 553–559 (2010).
25 Zou, Y., Lin, D., Dai, L. & Zhang, J. Synthesis of graft copolymer by coupling reaction of living poly (methyl methacrylate) with bromomethylated polystyrene. *Polymer* **39,** 2665–2668 (1998).
26 Zhang, X., Wang, P., Zhu, P., Ye, C. & Xi, F. Second, order non-linear optical materials based on poly (*p*-chloromethyl styrene). *Macromol. Chem. Phys.* **201,** 1853–1857 (2000).
27 Abbasian, M., Namazi, H. & Entezami, A. A. 'Living' radical graft polymerization of styrene to styrene butadiene rubber (SBR) with 2,2,6,6-tetramethyl-1-piperidinyloxy (TEMPO). *Polym. Adv. Technol.* **15,** 606–611 (2004).
28 Janata, M., Masar, B., Toman, L., Vlcek, P., Policka, P., Brus, J. & Holler, P. Multifunctional ATRP macroinitiators for the synthesis of graft copolymers. *Reac. Funct. Polym.* **50,** 67–75 (2001).
29 Endo, K. & Senoo, K. Syndiospecific copolymerization of styrene with styrene macromonomer bearing terminal styryl group by $CpTiCl_3$–methylaluminoxane catalyst. *Polymer* **40,** 5977–5980 (1999).
30 Yu, Z. Z., Yang, M., Zhang, Q., Zhao, C. & Mai, Y. W. Dispersion and distribution of organically modified montmorillonite in nylon-66 matrix. *J. Polym. Sci. Part B Polym. Phys.* **41,** 1234–1243 (2003).
31 Wang, K., Liang, S., Du, R., Zhang, Q. & Fu, Q. The interplay of thermodynamics and shear on the dispersion of polymer nanocomposite. *Polymer* **45,** 7953–7960 (2004).
32 Morgan, A. B. & Gilman, J. W. Characterization of polymer-layered silicate (clay) nanocomposites by transmission electron microscopy and X-ray diffraction: a comparative study. *J. Appl. Polym. Sci.* **87,** 1329–1338 (2003).
33 Kim, Y., Koo, B. H. & Do, Y. Synthesis and polymerization behavior of various substituted indenyl titanium complexes as catalysts for syndiotactic polystyrene. *J. Organomet. Chem.* **527,** 155–161 (1997).
34 Costantino, U., Gallipoli, A., Nocchetti, M., Gamino, G., Bellucci, F. & Frache, A. New nanocomposites constituted of polyethylene and organoclly modified ZnAl hydrotalcites. *Polym. Degrad. Stabil.* **90,** 586–590 (2005).
35 Chen, W. & Qu, Q. LLDPE/ZnAl LDH–exfoliated nanocomposites: effects of nanolayers on thermal and mechanical properties. *J. Mater. Chem.* **14,** 1705–1710 (2004).